Infrared Spectroscopy Experiment for Mariner Mars 1971[1]

R. A. HANEL, B. J. CONRATH. W. A. HOVIS. V. KUNDE,
P. D. LOWMAN, C. PRABHAKARA, AND B. SCHLACHMAN

Laboratory for Atmospheric and Biological Sciences. Goddard Space Flight Center,
Greenbelt, Maryland

G. V. LEVIN

Biospherics, Inc., Rockville, Maryland 20850

Received March 24, 1969; Revised August 4, 1969

The infrared interferometer spectrometer to be carried on the Mariner Mars 1971 mission is a Michelson interferometer operating in the spectral range 200 to 1600 cm^{-1}, with an apodized spectral resolution corresponding to 2.4 cm^{-1}. Use of the instrument on a Mars-orbiting spacecraft provides an opportunity for inferring spatial and temporal behavior of various physical parameters associated with the planetary atmosphere and surface. Included among these parameters are atmospheric and surface temperatures and total atmospheric water vapor content. A search can be made for minor atmospheric constituents that are optically active in the spectral range of the observations. Information on the types of surface materials present can be obtained from the phenomenon of *reststrahlen*, and analyses of cooling curves should also be useful in surface studies. To illustrate the information content of the interferometer measurements, examples of synthetic spectra calculated by using model atmospheres are given. Techniques for obtaining the various physical parameters from measured spectra are discussed. Preliminary analysis indicates that water vapor amounts as low as 0.1 precipitable micron should he detectable under reasonable assumptions on the behavior of the atmospheric temperature profile. The inferred parameters should provide essential input for studies of the physical behavior of the atmosphere, such as the nature of the general circulation. Of considerable biological interest are the possible implications of the measurements for the existence or nonexistence of water in the liquid phase. The identification of surface materials and of minor atmospheric constituents may also contribute to biological studies.

I. INTRODUCTION

The thermal emission spectrum of a planet depends on many atmospheric and surface parameters. The most important atmospheric parameters are the types of optically active gases present, the abundance and distribution of these gases. and the temperature profile; the most important surface parameters are temperature, pressure. composition, and structure.

[1]This work was performed for the Jet Propulsion Laboratory, California Institute of Technology, sponsored by the National Aeronautics and Space Administration, under Contract No. NAS-7-100.

The infrared spectroscopy (IRIS M) experiment for Mariner Mars 1971 is designed to provide spectral measurements of the thermal emission of the Martian surface and atmosphere. The spectral range covered is 200 to 1600 cm^{-1} with 2.4-cm^{-1}-wide spectral resolution elements. Spatial resolution is approximately 126 km for an altitude of 1600 km The orbital mission allows the Martian atmospheric and surface properties to be studied with respect to geographic location and time variation.

Absorption features due to polyatoinic molecules lie within the measured spectral range. To date, only CO_2 (Owen, 1966; Spinrad *et al.*, 1966; Belton *et al.*, 1968; Giver *et al.*, 1968), H_2O (Kaplan *et al.*, 1964; Schorn *et al.*, 1967) and CO (Connes, 1968) have been positively identified by spectroscopic means in the Martian atmosphere. A tentative identification of O_2 has been made by Belton and Hunten (1968) from two weak absorption lines of the oxygen A band. Analysis of these lines yields an O_2 abundance of 20 cm-atm or less. The strongly absorbing spectral region centered near 667 cm^{-1} due to carbon dioxide will provide information on the vertical temperature distribution in the atmosphere; the more nearly transparent portions of the spectrum will be well suited for the search for minor atmospheric constituents and for the possible observations of reststrahlen phenomena caused by minerals in the Martian surface.

II. SCIENTIFIC OBJECTIVES

The basic scientific objectives of the experiment are to utilize measurements of the spectral radiance $I(\nu)$ of the thermally emitted radiation from the Martian atmosphere and surface to infer atmospheric and surface parameters. These parameters will then be used in studies of the physical behavior of the atmosphere, investigations of the surface composition and structure, and biological studies.

To obtain some feeling for the quantities to which such measurements are sensitive, it is instructive to consider the theoretical expression for $I(\nu)$, which can be written as follows:

$$I(\nu) = \epsilon(\nu)\, B(\nu, T_s)\, \tau_s(\nu) - \int_{\log P_t}^{\log P_s} B[\nu, T(\log P)] \frac{\partial \tau(\nu, \log P)}{\partial \log P} d \log P. \quad (1)$$

$B(\nu, T)$ is the Planck intensity at wave number ν and temperature T, and the transmittance for the atmospheric gas between pressure level P and the effective top of the atmosphere P_t is represented by $\tau(\nu, \log P)$. The subscript s refers to surface values, and $\varepsilon(\nu)$ represents the emissivity of the planetary surface. The atmosphere is assumed to be in local thermodynamic equilibrium, and the small contribution to $I(\nu)$ from radiation reflected from the surface has been neglected. The first term in Eq. (1) represents the thermal emission from the surface, attenuated by the atmosphere, and is dependent on the surface emissivity and surface temperature as well as the total atmospheric transmittance. The second term represents the atmospheric emission and is dependent on the atmospheric temperature profile through the source function $B[\nu, T(\log P)]$ and on the type, total amount, and vertical distribution of the optically active gases through transmittance $\tau(\nu, \log P)$.

Techniques for inferring the various physical parameters from measurements of $I(\nu)$ and their applications to surface, atmospheric, and biological studies are considered in the following paragraphs.

III. DISCUSSION

1. *Atmosphere*

To illustrate the information contained in the type of measurements anticipated from the experiment, several synthetic spectra have been calculated using Eq. (1) and assuming model Martian atmospheres. Figure 1 shows the results of such calculations for the spectral region in the vicinity of the 667-cm^{-1} absorption band of CO_2. For this illustration, a temperature profile based on calculations of radiative and convective equilibrium by Gierasch and Goody (1968) was used. The profile, which is for equinox conditions at the equator at 16:00 hr local time, possesses a "discontinuity" of 36°K across a 10-m-thick boundary layer at the surface. Since the Gierasch-Goody calculations extend to 30 km only, the temperature profile was extrapolated isothermally above that level. A surface pressure of 5 nib was employed, and the chemical composition was taken as essentially pure CO_2 (68 rn-atm). The surface emissivity $\varepsilon(\nu)$ was set equal to unity for all ν in this case.

In calculating the values of $\tau(\nu, \log P)$ required in Eq. (1), the monochromatic molecular absorption coefficient along the atmospheric slant path was determined by summing the contribution of all individual lines at a particular frequency using theoretically calculated line positions and strengths. The spectral integration techniques used have been described previously (Kunde, 1968 *a,b*). The theoretical molecular line parameters for the 667-cm^{-1} carbon dioxide band were obtained from Drayson and Young (1967). The effect was included of a triangular instrument function of 2-cm^{-1} total width at half maximum. Figure 1 shows the resulting synthetic spectra expressed in terms of the brightness temperatures corresponding to the calculated radiances. Spectra corresponding to the contributions of the various isotopic species are shown, as well as the complete spectrum including all isotopes. The isotopes were weighted by their relative terrestrial abundances.

The Q branches of the fundamental and strong combination bands are evident in the spectra as is the rotational structure of some of the bands. For identification purposes, the observed spectra will exhibit even more line structure than shown in Fig. 1, as the unapodized spectra expected from the instrument correspond to a higher

spectral resolution of 1.2 cm^{-1}. Qualitatively, the general shape of the temperature profile in the region of the $^{12}C^{16}O_2$ Q branch (667 cm^{-1}) absorption can be determined by observing the shape of the Q branch in the spectrum. Contributions to the radiances in the strongly absorbing Q branch come from relatively high in the atmosphere. On Earth, most of the absorption and subsequent reemission occurs in the stratosphere where the temperature is increasing with altitude, resulting in a higher brightness temperature for the Q branch region with respect to the adjacent portion of the spectrum. For the Mars model, contributions from the higher portions of the atmosphere correspond to cooler temperatures, and the minimum brightness temperature occurs in the Q branch region. Thus, the 667-cm^{-1} Q branch qualitatively indicates whether the temperature is increasing or decreasing in the region of Q branch absorption.

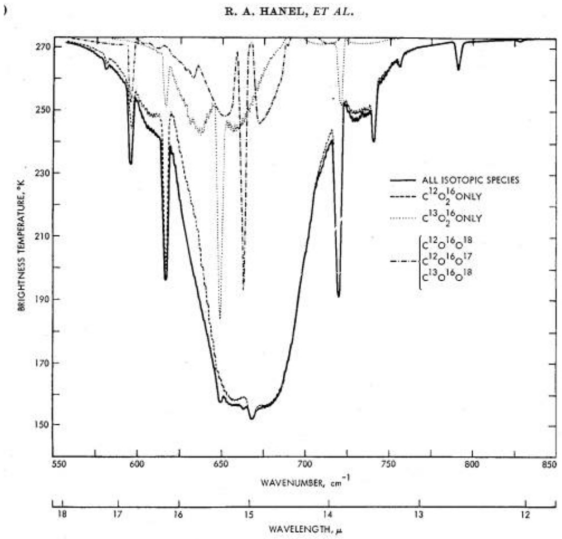

FIG. 1. Synthetic brightness temperature spectra for the 667-cm^{-1} CO_2 absorption band.

To obtain quantitative information on the temperature profile throughout the atmosphere, more complex considerations are required. A considerable literature exists on computational techniques for obtaining temperature profiles from remote radiometric measurements (Wark, 1961; Yamamoto, 1961; Twomey, 1963, 1965; King. 1964; Wark and Fleming, 1966; Conrath, 1968. The principle of obtaining temperature profiles from observed spectra can be understood by considering the atmospheric term in Eq. (1). The factor $|\partial\tau(\nu, \log P/\partial \log P|$ can be regarded as the weight given the source function $B[\nu, T(\log P)]$ at each level P. Figure 2 shows weighting functions for several different wavenumbers calculated using the model atmosphere discussed above. Because the principal levels of contribution move from higher to lower levels in the atmosphere in moving from the opaque band center to the less opaque band wings, measurements across an absorption band permit a reconstruct ion of the temperature profile. Considerable overlap of the weighting functions causes solutions obtained for the temperature profile to be sensitive to instrumental noise, and considerable effort has been expended in developing techniques that will provide stability by introducing smoothing constraints into the solutions.

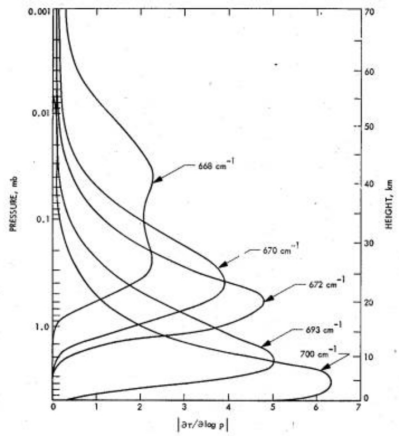

FIG. 2. Sample weighting functions for the 667-cm^{-1} carbon dioxide band. An essentially pure CO_2 (68 m-atm) atmosphere with a 5-mb surface pressure was assumed, and spectral resolution elements 2 cm^{-1} wide were used. The examples shown give an indication of the height range over which information on the temperature profile can be obtained.

Temperature profiles have been successfully recovered from data obtained for the Earth's atmosphere (Hanel and Conrath, 1969). An example of data from the IRIS "B" instrument covering the spectral range 400 to 1400 cm^{-1} with spectral resolution elements 5 cm^{-1} wide is shown in Fig. 3. The temperature and water vapor mixing ratio profiles inferred from these data are shown in Fig. 4 and 5, respectively, along with "radiosonde" data taken at a nearby station for comparison. Computational techniques developed for application to data from the Earth's atmosphere are adaptable to the Martian case in a general sense, although considerable work is necessary for the specific application.

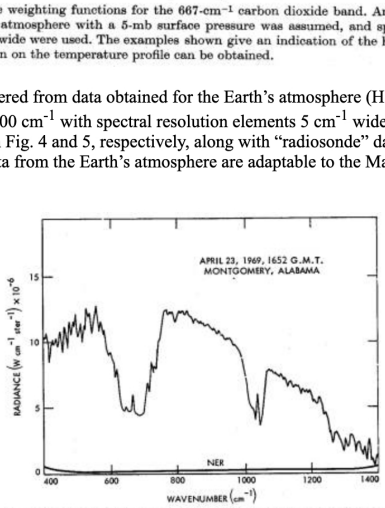

FIG. 3. Spectrum of the terrestrial atmosphere obtained with the IRIS "B" instrument on Nimbus III. This version of the instrument covered the spectral range between 400 and 2000 cm^{-1} with spectral resolution elements 5 cm^{-1} wide. The curve just above the abscissa is the noise equivalent radiance (NER).

In order to properly interpret the observed spectrum and to obtain the correct temperature profile, it is necessary to have accurate values of the carbon dioxide mixing ratio and the surface pressure. The curve-of-growth techniques utilized in the near-infrared cannot be applied to the thermal emission spectra directly because of the additional complication of the source function. The possibility of using differential pressure effects in the 667-cm^{-1} CO_2 band as a means for estimating the surface

pressure and CO_2 mixing ratio is currently being investigated. Should this approach prove to be unfeasible, ground-based values or values derived from the occultation experiment will be used. It will, of course, be possible to check these values, along with the other inferred atmospheric parameters, for internal consistency by comparison of a synthetic spectrum with the observed spectrum.

Among the possible minor atmospheric constituents, water vapor is of primary interest because of its biological as well as its geological importance. In order to obtain an estimate for the sensitivity of the anticipated spectral measurements to the total water vapor content in an atmospheric column, synthetic spectra have been calculated for the region of rotational water vapor absorption between 200 and 600 cm^{-1}. The same atmospheric temperature profile was used as in the calculations of the CO_2 spectra described previously, and a constant water vapor mixing ratio was assumed. The positions and strengths of the rotational water vapor lines were obtained from Benedict (1968), and spectral resolution elements 2 cm^{-1} wide were again employed. Figure 6a shows the resulting brightness temperature spectra for total water vapor contents of 14.6 precipitable micron and for 0.1 precipitable micron. For the 0.1-precipitable-micron water vapor content, the brightness temperature fluctuation is approximately 1°K, which corresponds to a radiance fluctuation 4.5 x 10^{-8} W cm^{-1} $sterad^{-1}$. The noise level of the IRIS M instrument is expected to be of that order, so a 0.1 precipitable micron of water vapor represents a signal corresponding to the noise level. The detectability can be improved by averaging several spectra together.

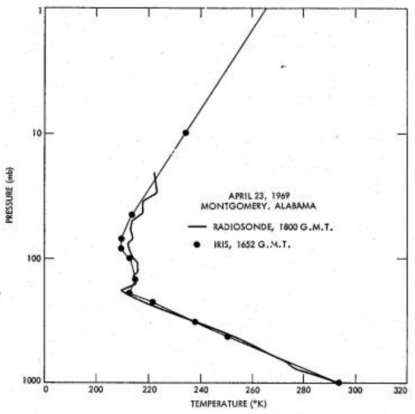

FIG. 4. Terrestrial temperature profile obtained from the measured spectrum shown in Fig. 3. A temperature profile based on data obtained from a nearby radiosonde station is shown for comparison.

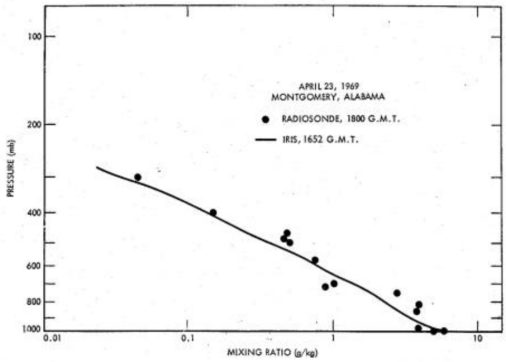

FIG. 5. Water vapor mixing ratios derived from the measured spectrum shown in Fig. 3. Radiosonde data taken nearby permit comparison.

The sensitivity of the measurements to total water vapor content depends on the behavior of the atmospheric temperature relative to the surface temperature. The rotational H_2O spectrum was also computed without the 36°K boundary-layer "discontinuity," with the results shown in Fig. 6b. The changes in brightness temperature, due to the presence of a 0.1 precipitable micron of water vapor, are approximately 0.5°K. Removal of the temperature "discontinuity," therefore, decreases the apparent strength of the water vapor absorption features by a factor of only about 2.

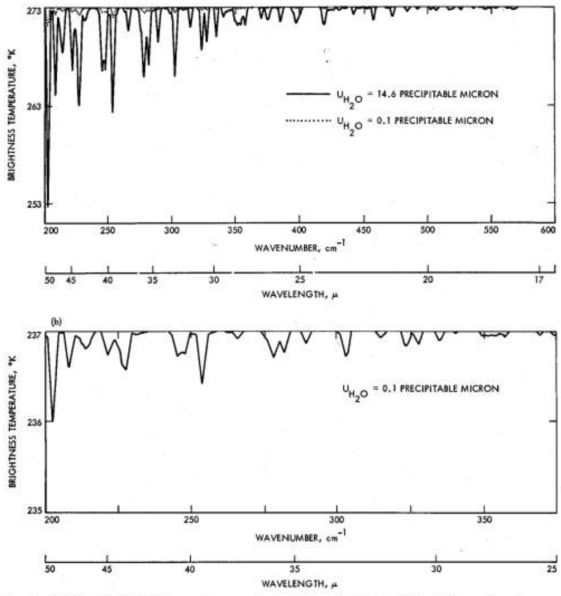

FIG. 6. (*a*) Synthetic brightness temperature spectra for the rotational lines of water vapor. Spectra calculated assuming water vapor contents of 14.6 precipitable micron and 0.1 precipitable micron with a boundary layer temperature "discontinuity" of 36°K. (*b*) Spectrum calculated for 0.1 precipitable micron water vapor content without the boundary-layer temperature "discontinuity".

In addition to water vapor, the presence of other minor atmospheric constituents is of interest, since their presence reflects on the evolution of the atmosphere and may also be indicative of biological activity. The various possible minor constituents on Mars for which upper abundance limits have been determined are listed in Table

I. In most cases, the upper limits were deduced from the absence of absorption lines or bands in the observed spectra. The search for minor constituents, such as those listed in Table I, must be based in part on a compilation and study of laboratory spectra of the gases involved. In addition, systematic procedures must be developed for predicting abundances in a self-consistent fashion from thermodynamic, chemical, and photochemical equilibrium considerations. Several recent investigations show the type of procedure required, even though some of their results are now outdated. Considering thermodynamic and photochemical equilibrium for nitrogen oxides on Mars, along with the upper limits for O_2 and NO, Sagan, Hanst, and Young (1965) have theoretically reduced the upper limit for the abundance of NO_2 below its previously observed value. Lippincott, Eck, Dayhoff, and Sagan (1967) reduced the equilibrium upper limit of NO_2 several orders of magnitude below the value of Sagan *et al.* In their investigations, Lippincott *et al.* included a larger number of equilibrium reactions than Sagan *et al.*, but considered only chemical equilibrium. The initial CO_2 mixing ratio used by Lippincott *et al.* was 0.10, which is considerably lower than current best estimates. so their results can no longer be considered quantitatively valid. Bortner and Alvea (1968) have calculated the steady state concentrations of 18 species as a function of altitude in the Martian atmosphere. Investigations of the type mentioned are valuable as a guide in the search for minor constituents, and should be extended to include as many chemical reactions as possible.

TABLE I

UPPER LIMITS ON ABUNDANCES FOR POSSIBLE MINOR CONSTITUENTS IN THE MARTIAN ATMOSPHERE

Molecule	Path length (cm-atm)	References
O_3	0.004	Belton and Hunten, 1968
NO	20	Kuiper, 1964
NO_2	0.0008	Marshall, 1964
N_2O	0.08	Kuiper, 1964
NHO_2	0.16	Sagan, Hanst, and Young, 1965
HCHO	0.3	Kuiper, 1964
COS	0.2	Kuiper, 1964
H_2S	7.5	Kuiper, 1964
CH_4	0.1	Kuiper, 1964
C_2H_4	3	Kuiper, 1952
C_2H_6	1	Kuiper, 1952
NH_3	0.1	Kuiper, 1964

In most cases, the concentrations of minor constituents can be expected to be sufficiently small so that it will be difficult to directly recognize the spectral features of the gases in the measurements. In these cases, techniques will have to be utilized for improving the effective signal-to-noise ratio such as averaging a number of spectra together and using cross-correlation analysis. In the latter approach, the cross-correlation $c(\nu)$ is formed between the known spectrum of the gas to be identified $T(\nu)$ and the measured brightness temperature spectrum $\check{T}(\nu)$

$$c(\nu) = \int T(\nu')\check{T}(\nu + \nu')\,d\nu'. \qquad (2)$$

A significant peaking of $c(\nu)$ at zero lag would he indicative of the presence of the gas in question.

One example of the possible uses of the parameters derivable from the thermal emission spectra is a study of the general circulation of Mars. The lack of appreciable amounts of water vapor and bodies of liquid water will tend to simplify the general circulation of Mars compared with that of Earth. On the other hand, the possible freezing of CO_2 at the winter pole (Leighton and Murray, 1966) may complicate the flow patterns. An investigation of the Martian circulation may be made with numerical models (e.g., Leovy and Mintz, 1966) or analytical techniques (Gierasch and Goody, 1968). Studies are continuing on the general circulation and possible correlations with the wave of darkening, inquiries into the composition of the polar caps. and other branches of investigation using the data anticipated from this instrument.

2. *Surface*

For studies of the Martian surface, it is necessary to choose spectral intervals where the atmosphere is nearly transparent, so the first term in Eq. (1) is dominant. Such atmospheric "windows" exist in the 8 to 13 μ region and in some portions of the region from 18 to 50 μ (Kunde, 1967). If the surface emissivity $e(\nu)$ possesses distinct features in these spectral intervals, then it may be possible to identify the type of material present.

The phenomenon of reststrahlen in some minerals produces variations in $\varepsilon(\nu)$ within the observable spectral interval. This phenomenon was first noticed by optical physicists in the reflectance spectra of polished crystalline minerals such as quartz, salt, and corundum. The marked increase of reflectance in certain wavelengths longer than 8 μ was used to localize the areas of the spectrum where the resstrahlen bands occurred. Recently, this optical phenomenon has been revived for remote sensing. Measurements by several investigators (Hovis and Callahan, 1966; Lyon, 1965) have shown that the resstrahlen of silicate-bearing minerals varies in wavenumber with the concentration of the silicate. Igneous rocks are often classified by the SiO_2 content. Granite with more than 65% SiO_2 is considered acidic; dunite, with less than 45% SiO_2, is considered ultrabasic.

Figure 7 shows the measured reststrahlen of four typical igneous rocks for four fractured, but unpolished, solid samples. As can be seen, the peak of the various reststrahlen varies from about 8.5 to about 11 μ, with the most acidic having the peak at shortest wavelength. Though there is no satisfactory theoretical explanation for this behavior, many measurements have found no exceptions. As the material is ground to smaller sizes, there is a weakening of the reststrahlen features (see Fig. 8). Though the reststrahlen remain, they are considerably weaker in the smaller particles; thus, they require greater instrumental accuracy for detection than do the larger solid samples.

The investigations of reststrahlen mentioned were restricted to wavenumbers greater than approximately 455 cm^{-1}. The spectroscopic work of Aronson, Emslie, Allen, and McLinden (1966) on minerals indicates that considerable information on surface composition can also be obtained from the spectral region below 455 cm^{-1}.

Cooling curves can provide another means of acquiring information on the nature of the surface materials. Ideally, one would like to obtain the surface temperature at a particular location as a function of local time through a complete day-night cycle. In practice, it will be difficult to obtain such data for one small surface area, but it should be possible to obtain measurements from various points on relatively homogeneous surface features intersected by the terminator. Computational techniques have been developed for obtaining the parameter $(kpc)^{-1/2}$ from the cooling curves, where k, p, and c are, respectively, the thermal conductivity, density, and specific heat of the surface material (Wesselink, 1948; Jaeger, 1953).

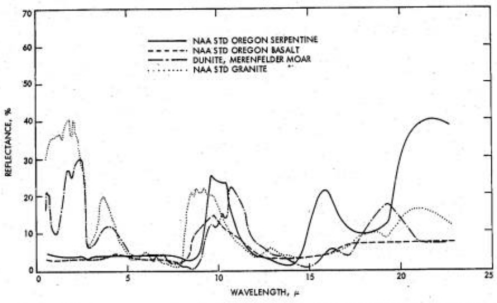

FIG. 7. Measured reflectance spectra of solid, fractured rock samples displaying the phenomenon of reststrahlen.

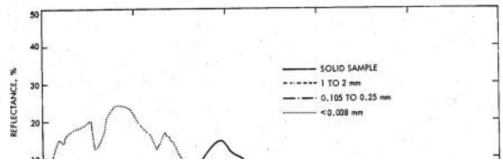

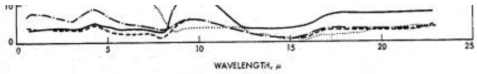

FIG. 8. Measured reflectance spectra of solid and ground basalt. The weakening of the reststrahlen features, as the material is ground to smaller sizes, is illustrated.

3. *Biological Inferences*

Observations of various atmospheric and surface parameters will provide a basis for biological inferences. The problem of whether it is possible in principle for water to exist in the liquid phase at the planetary surface is of primary concern. Therefore, it is highly important to obtain accurate determinations of the surface temperature, water vapor concentration, and the total atmospheric pressure at many locations. The maximum brightness temperature observed in the high-resolution spectra will provide a better estimate for the surface temperature than can generally be obtained from broad-band radiometric measurements.

IRIS data from specific surface features, such as the regions near the polar caps, may be compared with data from the same features obtained with the infrared radiometer, television, and the ultraviolet spectrometer. Consideration will be given to the possibility that areas of vegetation may provide identifiable spectral features, and if this should prove to be true, comparisons of IRIS spectra with spectra of selected terrestrial compounds can be made.

Observations of minor atmospheric constituents may be indicative of biological activity. In particular, studies of the temporal and spatial distribution of water vapor or other gases on a planetary scale may provide some indication of the most likely periods of time and the locations for which biological processes may be most active.

IV. INSTRUMENTATION

The proposed instrument is a Michelson interferometer which is in all critical areas (detector, beamsplitter, auxiliary interferometer, calibration, and large parts of the electronic circuitry) identical to the interferometer designed for the Nimbus B and D meteorological satellites. Some of the mechanical and electrical configurations and circuits will be changed for two reasons: (1) the interface with the existing Mariner spacecraft and its power and data-handling systems will require some modifications to the instrument; and (2) the experience gained in extensive testing of the Nimbus instruments suggests several improvements, which permit an increase in spectral resolution to become equivalent 2.4 cm^{-1} in the apodized spectra and to 1.2 cm^{-1} in the unapodized one. This increase in resolution is considered significant. It will allow the recognition of individual lines in the rotation-vibration CO_2 bands, which are spaced at approximately 1.6 cm^{-1}.

1. *The Design*

Table II summarizes the more important parameters of the Nimbus interferometers and the Mariner Mars 1971 instrument (IRIS M). Figure 9 is a simplified diagram of the proposed instrument.

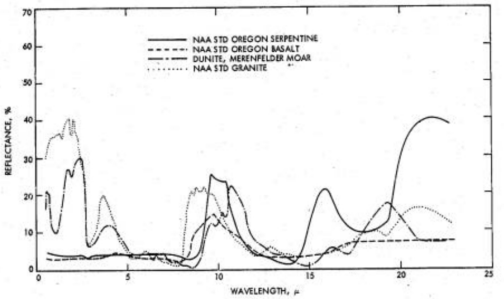

FIG. 7. Measured reflectance spectra of solid, fractured rock samples displaying the phenomenon of reststrahlen.

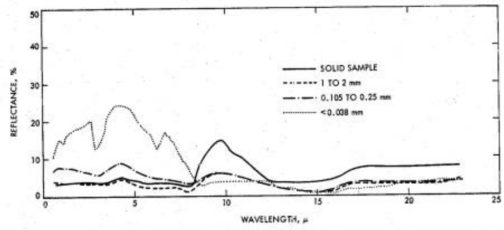

FIG. 8. Measured reflectance spectra of solid and ground basalt. The weakening of the reststrahlen features, as the material is ground to smaller sizes, is illustrated.

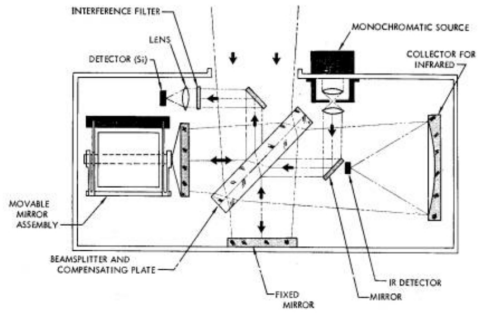

FIG. 9. Simplified diagram of Michelson-type interferometer. The reference source is a near-infrared line of a neon discharge tube.

The essential part of the interferometer is the beamsplitter, which divides the incoming radiation into two approximately equal components. After reflection from the fixed and moving mirrors, respectively, the two beams interfere with each other with a phase difference proportional to the optical path difference between both beams. The recombined components are then focused onto the detector where the intensity is recorded as a function of path difference, δ. Since the mirror motion is phase-locked to a stable clock frequency, the mirror path difference is also proportional to time. For quasi-monochromatic radiation, a circular fringe pattern appears at the focal plane of the condensing mirror. There the detector size is chosen to cover just the smallest central fringe for the highest wavenumber of interest. This aperture also determines the field of view of the instrument.

The central fringe may be light or dark depending on the path difference between the two beams. For polychromatic radiation and neglecting constant terms, the signal at the detector, called the interferogram, is

$$i(\delta) = \int_0^\infty K_\nu (B_\nu - B_i) \cos(2\pi\nu\delta - \phi_\nu) d\nu.$$

The amplitude is proportional to a responsivity factor K_v and the difference in radiance between the scene within the field of view B_v, and B_i. the Planck function corresponding to the instrument temperature. The phase is defined with respect to a point chosen as close as possible to, but not necessarily at, the zero path difference point. Imperfect optical compensation and residual phase shift in the analog part of the data channel cause the angle ø to depend somewhat on the wavenumber. Reconstruction of the spectrum is performed on the ground by a digital computer.

The cesium iodide beamsplitter of the Mariner instrument is optically flat to a fraction of a visible fringe. It has a multilayer dielectric coating, which is optimized to the 6 to 50 μ region except for a small area in the center where the beamsplitter is coated to perform well in the visible and near-infrared. In this center region, the fringe control interferometer operates. It not only utilizes the same beamsplitter, but also the prime infrared interferometer mirrors. The fringe control interferometer generates a sine wave of 675 Hz at the detector from a nearly monochromatic spectral line of a low-pressure neon discharge lamp. The line is isolated by an interference filter. The 675-Hz signal serves, after being divided by 3, as a sample command and ensures equal distance sampling; it is compared in phase to a clock frequency to provide the error signal for the phase-locked loop.

The Michelson mirror assembly has an electromagnetic drive coil and also a pickup coil to generate a voltage proportional to mirror velocity. The velocity signal is also used in a feedback arrangement to provide electrical damping and to make the system insensitive to moderate levels of external vibration. The phase-locked condition of the Michelson mirror provides a constant mirror velocity and permits a constant data rate; moreover, the data stream can be synchronized with the spacecraft clock.

The image motion compensation and calibration system channels radiation from several sources to the interferometer. After seven interferograms are taken in the operating mode, one is taken from a built-in, warm blackbody (290°K) followed by another set of seven planetary interferograms and finally by an interferogram from the interstellar background (4°K). The spectra from the blackbody and from space serve calibration purposes to be discussed later.

The instrument generates main data and housekeeping data. The main data are quantized in a 11-bit analog-to-digital converter. A 12th bit indicates the position of a gain control switch. Sixty-four words of housekeeping information (blackbody temperature, voltages, etc.) are transmitted immediately before and immediately after each interferogram. The total number of bits per frame is then 50 688.

Some of the housekeeping data are multiplied with the main data and are then transmitted just before and just after each interferogram. This set of housekeeping data is required in the data reduction process. Another set of housekeeping data for instrument performance evaluation is transmitted via the spacecraft system.

2. *Data Reduction in Ground-Based Computer*

The data reduction process consists of four steps:

(1) A check of consistency and completeness of input tape and processing of housekeeping information.

(2) Fourier transformation of all interferograms by the Cooley-Tukey method.

(3) Phase correction, and application of calibration procedure.

(4) Production of output tapes that contain the calibrated spectra, housekeeping information, and orbital parameters.

In the check of consistency and completeness, the total number of words per interferogram is determined. Housekeeping data are converted into engineering units such as temperatures by application of conversion tables established during preflight calibrations.

Spectra that pass the screening procedure mentioned above will then be transformed, corrected in phase, and submitted to the calibration procedure.

3. *Calibration*

The instrument is exposed occasionally to a built-in calibration blackbody and to outer space, by rotation of the image motion compensation mirror.

The calibration spectra are transformed in the same manner as the spectra obtained while viewing Mars. The amplitude c_v, in the spectrum is proportional to the difference in radiance between the instrument and the target

$$c_v = r_v(B_{\text{target}} - B_{\text{instrument}}).$$

The factor of proportionality is the responsivity of the instrument.

One obtains a set of three equations: one for the target (index 1), one for the cold blackbody (index 2), and one for the warm blackbody (index 3). Under the assumptions that the responsivity, r_v, is independent of the target brightness and that the detection and amplification is a linear process, the three equations may be solved to yield B_1 as well as r_v and B_i. If one uses the interstellar background as the cold reference (~4ºK), then B_2 is, for all practical purposes, zero, and the equations simplify to

$$B_1 = B_3\frac{C_2 - C_1}{C_2 - C_3}$$
$$r_v = \frac{C_2 - C_3}{-B_3}$$
$$B_i = B_3\frac{C_2}{C_2 - C_3}.$$

The equation for B_1 is used to reduce the spectra. Neither the responsivity nor the instrument temperature are contained explicitly in this equation. The calibration spectra C_2 and C_3 are the average of many individual spectra so that the random effects in these spectra are greatly reduced. Then the sample standard deviation s_v, of the responsivity is determined for each orbit

$$s_v = \left[\sum_{i=1}^{k}(r_v - \bar{r}_v)^2/(k-1)\right]^{1/2}.$$

The r_i are the responsivities computed from each calibration pair (hot and cold black-bodies). The average responsivity per orbit is called r_v. and k is the number of calibration pairs per orbit. The standard deviation gives the short-time repeatability of the instrument and allows a judgement of the magnitude of the random errors in each spectral interval. The noise equivalent radiance may be calculated from

$$\text{NER} = \sqrt{2}\, sB_3/\bar{r}_v.$$

A comparison of the mean orbital responsivity for each spectral interval from orbit to orbit, and from day to day yields the long-term drift.

The derived instrument temperature T_i, which is calculated from B_i, and the instrument temperature measured by the thermistors embedded in the housing should be in close agreement. A deviation from this agreement is used as a caution flag, which requires a special investigation if it should occur.

V. SUMMARY

The infrared spectroscopy experiment will provide information on a wide range of physical parameters associated with the Martian atmosphere and surface. These data can be applied toward an understanding of many problems associated with the planet, such as the general circulation of the atmosphere, structure and composition of the surface, and the possible existence of biological activity. In the present report, it has been possible to give only rather general treatments of a few of the areas to which the experiment is applicable. Effort is currently being devoted to developing, in a more quantitative fashion, the various techniques required for extracting the desired physical parameters from the type of spectral data anticipated.

REFERENCES

ARONSON, J. R., EMSLIE. A. G., ALLEN. R. V., and McLINDEN. H. G. (1966). “Far Infrared Spectra of Silicate Minerals for Use in Remote Sensing of Lunar and Planetary Surfaces.” Final Report, Contract NAS 8-20132 to George C. Marshall Space Flight Center, NASA.

Planetary Surfaces." Final Report, Contract NAS 8-20122 to George C. Marshall Space Flight Center, NASA.
BELTON, M. J. S.. BROADFOOT, A. L., AND HUNTEN, D. M. (1968). Abundance and temperature of CO_2 on Mars during the 1967 opposition. *J. Geophys. Res.* **73**, 4795-4806.
BELTON, M. J. S., AND HUNTEN, D. M. (1968). A search for O_2 on Mars and Venus: A possible detection of oxygen in the atmospheres of Mars. *Astrophys. J.* **153**, 963-974.
BENEDICT, W. S. (1968). Private communication.
BORTNER, M., AND ALYEA, F. (1968). "Chemical Kinetics and Composition of the Mars Atmosphere." NASA TM X-33693. Marshall Space Flight Center, Huntsville, Alabama.
CONNES, P. (1968). Private communication.
CONRATH, B. J. (1968). Inverse problems in radiative transfer. A Review. *Proc. XVIII Astronaut. Congr.*, pp. 339-360.
DRAYSON, R. S., AND YOUNG, C. (1967). "The Frequencies and Intensities of Carbon Dioxide Absorption Lines Between 12 and 18 Microns." Technical Report 08183-1-T, Univ. of Michigan, Ann Arbor, Michigan.
GIERASCH, P., AND GOODY, R. (1968). A study of the thermal and dynamical structure of the Martian lower atmosphere. *Planet. Space Sci.* **16**, 615-646.
GIVER, L. P., INN, E. C. Y., MILLER. J. H., AND BOESE, R. W. (1968). The Martian CO_2 abundance from measurements in the 1.05 μ band. *Astrophys. J.* **153**, 285-289.
HANEL, R. A., and CONRATH, B. C. (1969). Preliminary results from the interferometer experiments on Nimbus III. *Science* **165**, 1258-1260.
HOVIS, W. A., AND CALLAHAN, W. R. (1966). Infrared reflectance of igneous rocks, tuffs and red sandstone from 0.5 to 22 microns. *J. Opt. Soc. Am.* **56**, 639.
JAEGER, J. C. (1953). Conduction of heat in a solid with periodic boundary conditions, with an application to the surface temperature of the Moon. *Proc. Cambridge Phil. Soc.* **49**, 355-359.
KAPLAN, L. D., MŰNCH, G., AND SPINRAD, H. (1964). An analysis of the spectrum of Mars. *Astrophys. J.*, **139**, 1-15.
KING, J. I. F. (1964). Inversion by slabs of varying thickness. *J. Atmos. Sci.* **21**, 324-326.
KUIPER, G. P. (1952). "Atmospheres of the Earth and Planets" (G. P. Kuiper, ed.), Chap. 12. Univ. of Chicago Press, Chicago, Illinois.
KUIPER, G. P. (1964). *Commun. Lunar Planet. Lab.* **2** (31), 79.
KUNDE, V. G. (1967). Theoretical computations of the outgoing infrared radiance from a planetary atmosphere. *NASA Tech. Note TND-4045*.
KUNDE, V. G. (1968*a*). Theoretical molecular line absorption of CO in late-type atmospheres. *Astrophys. J.* **153**, 435-450.
KUNDE, V. G. (1968*b*). Theoretical molecular line absorption of CO in late spectral type atmospheres. *NASA Tech. Note.* **TN D-4798**.
LEIGHTON, R. B., AND MURRAY, B. C. (1966). Behavior of carbon dioxide and other volatiles on Mars. *Science* **153**, 136-144.
LEOVY, C. B., AND MINTZ, Y. (1966). "A Numerical General Circulation Experiment for the Atmosphere of Mars." Memorandum RM-5110-NASA, Rand Corporation, Santa Monica, California.
LIPPINCOTT, E. R., ECK, R. V., DAYHOFF, M. O., AND SAGAN, C. (1967). Thermodynamic equilibria in planetary atmospheres. *Astrophys. J.* **147**, 753-764.
LYON, R. J. P. (1965). Analysis of rocks of spectral infrared emission (8 to 25 microns). *Econ. Geol.* **60**, 715.
MARSHALL, J. V. (1964). *Commun. Lunar Planet. Lab.* **2** (35), 167.
OWEN, T. (1966). The composition and surface pressure of the Martian atmosphere: Results from the 1965 opposition. *Astrophys. J.* **146**, 257-270.
SAGAN, C., HANST, P. L., AND YOUNG, A. T. (1965). Nitrogen oxides on Mars. *Planet Space Sci.* **13**, 73.
SCHORN, R. A., SPINRAD, H., MOORE, R. C., SMITH, H. J., AND GIVER, L. P. (1967). High-dispersion spectroscopic observations of Mars II. The water-vapor variations. *Astrophys. J.*, 743-752.
SPINRAD, H., SCHORN, R. A., MOORE, R., GIVER, L. P., AND SMITH, H. J. (1966). High-dispersion spectroscopic observations of Mars I. The CO_2 content and surface pressure. *Astrophys. J.* **146**, 331-338.
TWOMEY, S. (1963). On the numerical solution of fredholm integral equations of the first kind by inversion of the linear system produced by quadrature. *Machinery* **10**, 97-101.
TWOMEY, S. (1965). The application of numerical filtering to the solution of integral equations encountered in indirect sensing measurements. *J. of Franklin Institute* **229**, 95-109.
WARK, D. Q. (1961 . On indirect temperature soundings of the stratosphere from satellites. *J. Geophys. Res.* **60**, 77-82.
WARK, D. Q., AND FLEMING, H. E. (1966). Indirect measurements of atmospheric temperature profiles from satellites: I. Introduction. *Monthly Weather Rev.* **94**, 351-362.
WESSELINK, A. J. (1948). Heat conductivity and nature of the lunar surface material. *Bull. Astron. Inst. Netherlands* **10**, 351-363.
YAMAMOTO, G. (1961). Numerical method for estimating the stratospheric temperature distribution from satellite measurements in the CO_2 band. *J. Meteorol.* **18**, 581-588.